

# We are IntechOpen, the world's leading publisher of Open Access books Built by scientists, for scientists

**6,900**

Open access books available

**186,000**

International authors and editors

**200M**

Downloads

**154**

Countries delivered to

**TOP 1%**

most cited scientists

**12.2%**

Contributors from top 500 universities



**WEB OF SCIENCE™**

Selection of our books indexed in the Book Citation Index  
in Web of Science™ Core Collection (BKCI)

Interested in publishing with us?  
Contact [book.department@intechopen.com](mailto:book.department@intechopen.com)

Numbers displayed above are based on latest data collected.

For more information visit [www.intechopen.com](http://www.intechopen.com)



# Performance of Aqueous Ion Solution/Tube-Super Dielectric Material-Based Capacitors as a Function of Discharge Time

---

Steven M. Lombardo and Jonathan Phillips

Additional information is available at the end of the chapter

<http://dx.doi.org/10.5772/intechopen.71003>

---

## Abstract

The discharge time dependence of key parameters of electrostatic capacitors employing a dielectric composed of the oxide film formed on titanium via anodization, saturated with various aqueous ion solutions, that is tube-super dielectric materials (T-SDM), was thoroughly documented for the first time. The capacitance, dielectric constant, and energy density of novel paradigm supercapacitors (NPS) based on T-SDM saturated with various concentrations of  $\text{NaNO}_3$ ,  $\text{NH}_4\text{Cl}$ , or KOH were all found to roll-off with decreasing discharge time in a fashion well described by simple power law relations. In contrast, power density, also well described by a simple power law, was found to increase with decreasing discharge time, in fact nearly reaching  $100 \text{ W/cm}^3$  for both 30 wt% KOH and  $\text{NaNO}_3$  solution-based capacitors at 0.01 s, excellent performance for pulsed power. For all capacitors, the dielectric constant was tested, which was greater than  $10^5$  for discharge times  $>0.01$  s, confirming the materials are in fact T-SDM. The energy density for most of the capacitors was greater than  $80 \text{ J/cm}^3$  of dielectric at a discharge time of 100 s, once again demonstrating that these capacitors are competitive for energy storage not only with existing commercial supercapacitors but also with the best prototype carbon-based supercapacitors.

**Keywords:** supercapacitor, superdielectric material, anodized titania, electric energy storage

---

## 1. Introduction

High-pulsed electrical power is required for lasers, flash photography, spark ignition, spot welders, fusion reactors, kinetic weapon systems, rapid acceleration of electric vehicles, etc. Capacitors, generally electric double layer capacitors (EDLC), also known as supercapacitors,

---

are preferred for pulse power applications, because they provide far higher power electric pulses, per weight/volume, than batteries [1, 2]. Moreover, unlike batteries, capacitors are not damaged by providing pulsed power. This robust feature leads to their employment as power load levelers to extend battery life. For example, in satellites, systems designed to transfer high power demand from batteries to a parallel capacitor system can significantly increase battery and satellite lifetime.

Most research into increasing capacitor energy density is focused on developing graphene, the conductive material with the highest surface area ( $\sim 2600 \text{ m}^2/\text{g}$ ), electrodes for the next generation EDLC [3–7]. The theory suggests that capacitors with graphene electrodes could have an ultimate energy density of  $\sim 800 \text{ J/cm}^3$ , a value far less than the current generation commercial lithium ion battery ( $\sim 2200 \text{ J/cm}^3$ ). Notably, current commercial supercapacitors have an energy storage rating of  $< 50 \text{ J/cm}^3$ .

Recently, a new type of ‘supercapacitor’ was invented, NP supercapacitors (NPS) with energy density rivaling the best prototype EDLC, but based on an entirely different paradigm [8–14]. Unlike EDLC that gain energy density through the use of high surface area electrodes with low dielectric value, NPS use low surface area electrodes and dielectrics with remarkably high dielectric constants, specifically super dielectric materials (SDM), that is materials with dielectric values greater than  $10^5$ , although values  $> 10^{11}$  are reported. SDM are composed of an ‘active phase’, such as salt dissolved in a liquid, and an ‘inactive’ mechanical phase such as anodized titania, T-SDM [8, 9], high surface area porous refractory oxides, Powder-SDM [10–12], or even simple fabrics, Fabric-SDM [13], that hold the active phase in place. The theoretical basis of SDM [8, 9] is that in an electric field the ions in solution travel to create dipoles, which are far longer (ca.  $1 \mu\text{m}$ ) than those found in solid dielectrics (ca.  $10^{-4} \mu\text{m}$ ). It is the ‘field canceling’ effect of dipoles, proportional to length, which leads to increased capacitance, as per the classic model of dielectric behavior [15–17].

It is reasonable to label NPS, a new type of supercapacitor based on the energy storage values achieved, approx.  $400 \text{ J/cm}^3$  for T-SDM with aqueous NaCl solutions at very slow discharge rates, rivaling, perhaps surpassing, the best graphene-based EDLC prototypes [18–20]. One unresolved issue: NPS performance as a function of frequency. Given the theory of NPS requires micron scale ionic migration in a liquid to form giant dipoles, there should be significant performance degradation (‘roll-off’) with increasing frequency. That is, if not enough time is available in a charge cycle for dipoles to fully form via ion travel, the dielectric value, energy density, etc. will be reduced. Thus, it is important to directly test the performance of NPS as a function of frequency. Given the most likely application, power release over very short times, ca.  $0.05 \text{ s}$ , special attention should be paid to discharge rate dependence of power and energy.

The one study of NPS performance as a function of discharge time was on F-SDM, a variety not found to have particularly high energy density. Significant roll-off of all parameters with decreasing discharge period (roughly equivalent to increasing frequency) was documented. The roll-offs, all parameters, were well fit by simple power law relations over orders of magnitude of discharge time. In the present study, we employed the same method used in the earlier study to characterize performance as a function of discharge period of a variety of high energy density NPS, those employing anodized titania saturated with various aqueous free ion solutions. Once again, significant roll-off was observed as expected and the power

law relation was found. Still, even with the noted degradation, the performance at the time periods of interest (e.g. 0.05 s discharge) was better than any commercial supercapacitor and possibly any EDLC prototype. Notably, comparison with EDLC prototype performance was difficult as fitted data on time response of these capacitors are apparently nonexistent.

## 2. Experimental

The NP supercapacitors were constructed of anodized titania foils filled with various aqueous salt solutions. The remaining metal of the original titania was one electrode and a graphitic material served as the other electrode. The performance of these capacitors was characterized using standard galvanostat constant current protocols. All procedures are described below.

Anodization process—Titanium foil anodes (99.99% Sigma Aldrich), approx. 0.05 mm thick, were anodized, as described elsewhere [8, 9, 21–23], in an ethylene glycol solution containing small quantities of ammonium fluoride (0.25% w/w) and water (2.75% w/w), using a titanium cathode (2 cm distant from the anode) at a constant DC voltage of 40 V for 46 min. This process created a layer of cylindrical hollow titania tubes on the parent titanium, average length measured to be  $7.7\pm0.4\text{ }\mu\text{m}$  [24], but for purposes of conservative computation of energy density and all other parameters, assumed to be  $8\text{ }\mu\text{m}$  in length. The tube diameter was found to be approximately 90 nm, but that figure does not enter the computations. In prior studies employing a nearly identical protocol, but using different anodization time periods, the intent was to create anodized layers/tubes of various lengths in order to test the impact of tube length on dielectric value and energy density. In this study, the intent was to focus only on the impact of the liquid phase composition, thus all the matrix material, that is the anodized titania, was produced using a single protocol and produced nearly identical anodized layers. Typical tubes formed from this process are very regular in structure and densely packed together [8, 9, 23, 24]. They are all oriented with the long axis perpendicular to the surface of the parent foil. No effort was made to crystallize the tubes via a thermal treatment.

Assembly of capacitors—All the capacitors employed were a standard parallel plate construction, consisting of an electrode composed of the unanodized section of the original titania foil, the dielectric consisting of the anodized section ( $2\times1\text{ cm}$ ) filled with an free ion containing aqueous solution, and a positive electrode of Grafoil, a form of compressed graphite. The tubes in the anodized layer were filled with solution simply by placing them in a beaker filled with the solution for 50 min at room temperature. Three different ion precursors were used: sodium nitrate ( $\text{NaNO}_3$ ), ammonia chloride ( $\text{NH}_4\text{Cl}$ ), and potassium hydroxide (KOH). Capacitors were constructed from aqueous solutions of the three salts, specifically three weight percent concentrations of each salt, 10, 20, and 30%, for a total of nine capacitors. A ‘control study’ employing distilled water was run as well.

After the salt solution saturation, the capacitor had one electrode, the metallic component of the anodized titanium foil, and a compound dielectric in the form of the titania tubes filled with aqueous solution. Placing a Grafoil sheet ( $2\times1\text{ cm}$ ) on top of the open tube end of the anodized film completed the capacitor. Specifically, a rectangle of Grafoil (compressed natural graphite, 99.99% carbon [25, 26]) 0.3 mm thick was placed on top. The metallic part of the

anodized foil was connected to the negative terminal of the galvanostat, and the Grafoil sheet connected to the positive terminal. The final volume used in subsequent calculations was that of the dielectric section,  $8 \mu\text{m} \times 2 \text{ cm} \times 1 \text{ cm}$ . Greater detail is given elsewhere [24].

## 2.1. Electrical measurement

All parameters, including energy density, power density, capacitance, and dielectric values, were derived from ‘constant current’ galvanostat data (BioLogic Model SP 300 Galvanostat, Bio-Logic Science Instruments SAS, Claix, France). Operated in constant current charge/discharge mode over a selected voltage range (2.3–0.1 V), the data can be employed directly to determine capacitance as a function of voltage from the slope of voltage as a function of time, that is, for constant current:

$$C = \frac{dq}{dt} / \frac{dV}{dt} = I / \frac{dV}{dt}$$

Clearly for capacitance which is not a function of voltage, this equation predicts a perfect saw tooth voltage vs. time pattern. In fact, in this and earlier studies, it was found that the capacitance is a function of voltage, leading to ‘irregular wave forms’ [8–13]. As discussed in earlier work, this indicates that the capacitance is voltage dependent, specifically decreasing as voltage increases. For this reason, the capacitance reported herein is for the voltage region between 0.1 and  $\sim 0.8$  V. In this voltage regime, the voltage vs. time relationship was always found to be nearly linear for all discharge times greater than 0.001 s indicating constant capacitance over this voltage region. In all cases, it was found that capacitance decreases with increasing voltage as a function of discharge time. The shorter the discharge time the more pronounced the departure from constant capacitance (**Figure 1**).

Given the variability of capacitance with voltage, energy cannot be computed directly from ‘capacitance’, but it can be determined directly from the constant current data. Specifically, energy was determined from the integrated area under the total discharge curve (volt seconds) multiplied by the constant current. Power was determined by dividing the directly determined energy, by the time required, during discharge, for the voltage to go from the maximum to the minimum value. Energy and power density were then determined by dividing energy or power by the volume of the dielectric.

Methods to determine energy and power density that require the use of data ‘extrapolated’ beyond the voltage range actual measured can lead to severe errors, generally overestimates. For example, impedance spectroscopy measures the dielectric constant over a narrow voltage range, generally  $0 \pm 15$  mV [27, 28], and provides little reliable information about energy storage characteristics. Determining the energy storage/power production of most capacitors requires a collection of data over the full voltage operating range [29–31].

Galvanostats operated in the constant current mode do not permit selection of frequency. In order to obtain capacitance as a function of frequency, the current is changed. In essence increasing the current decreases the period required to charge/discharge. Hence, each capacitor was tested over

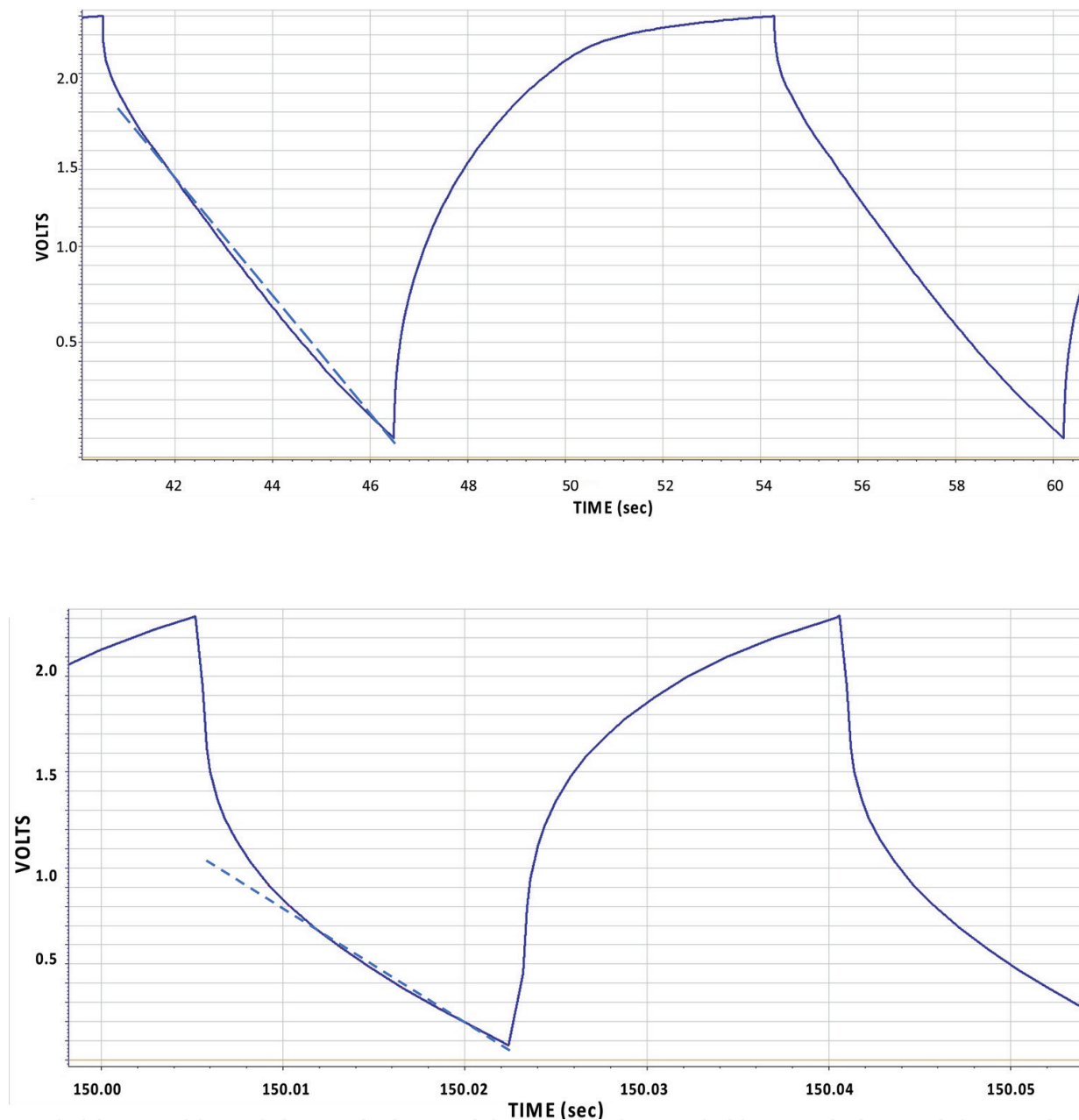


**Figure 1.** Deviation from voltage independent capacitance. (Top) For relatively long discharge times ( $>1$  s), the capacitance is nearly independent of voltage to nearly 2 V, as illustrated by the dashed line nearly matching data over a broad voltage range. (sample:  $\text{NH}_4\text{Cl}$  30%; charge rate: 10 mA). (Bottom) As the discharge time decreases, the deviation from ideal behavior, capacitance independent of voltage, becomes more pronounced (sample:  $\text{NH}_4\text{Cl}$  30%; charge rate: 100 mA). For all discharge times studied, the capacitance was nearly constant below 0.8 V.

a wide range of current values over the range 5–250 mA. In all cases, the charging current was the same magnitude as the discharge current, but of opposite sign. For each capacitor studied nine different currents in this range were used to determine capacitive behavior over approximately four orders of magnitude of the discharge time. At each selected constant current at least 10 complete cycles were recorded and generally 20. Averaged data from these cycles are reported. As noted, in all cases, the voltage was in the range 2.3–0.1 V. The finding that linear power law data

could fit the data collected in this fashion (see Results) demonstrates the efficacy of this method for determination of frequency response. An error analysis of this approach available elsewhere [13] suggests that all data for energy and power density is accurate to within 10% absolute.

### 3. Results

In brief, experiments were interpreted to yield information regarding the frequency dependence of these parameters: capacitance and dielectric values below 0.8 V, energy density, and power density over the range of 0.1–2.3 V. For all nine capacitors containing aqueous solutions with dissolved ions, but not the control using distilled water, the data permitted excellent power law fits to all parameters.

#### 3.1. Control

A capacitor employing distilled water as the electrolyte had such low values of relevant parameters that it was difficult to determine any parameters with precision, given the small capacitor size and the parameter ranges chosen for this study. A reliable power law ‘roll-off’ function was not obtained for any parameter as the absolute values were so small that the signal/noise ratio was large; however, it can be stated with certainty that the highest measured energy density was less than  $0.03 \text{ J/cm}^3$  clearly demonstrating that anodized titania-based T-SDM containing distilled water are not SDM.

#### 3.2. KOH

In order to illustrate general trends for all three solutes, the data on all three capacitors created with KOH-based SDM are presented in detail. The trends of energy and power density as well as dielectric and capacitance values determined below 0.8 V are shown on log-log plots, and in each case, it is clear that the data are well represented by simple power law relations over a wide range of discharge times.

Energy and power values are derived directly from data over the entire discharge voltage, thus may be considered as the most reliable. As shown in **Figure 2**, all the energy density data for KOH are well fit by simple power law relationships over four orders of magnitude of discharge time, that is from 20 to 0.002 s. Moreover, the curve fit is clearly of a quality that permits reasonable extrapolation to the energy density anticipated even for a 1000 s discharge. This value of energy density at this very slow discharge rate is suggested herein as a reasonable comparison point with battery energy densities (**Table 1**). It is notable that energy density is not a linear function of KOH concentration, but the 30 wt% sample was clearly superior.

Power density, following a trend observed previously for capacitors constructed with fabric-SDM (13), increases as the discharge time decreases. The data for the KOH SDM-based capacitors are shown in **Figure 3**. The trend shown was also found for SDM based on  $\text{NaNO}_3$  and  $\text{NH}_4\text{Cl}$  aqueous solutions. The absolute values are also very informative. For example, the capacitors can provide of the order  $100 \text{ W/cm}^3$  for discharges of 0.01 s, a remarkably high value appropriate

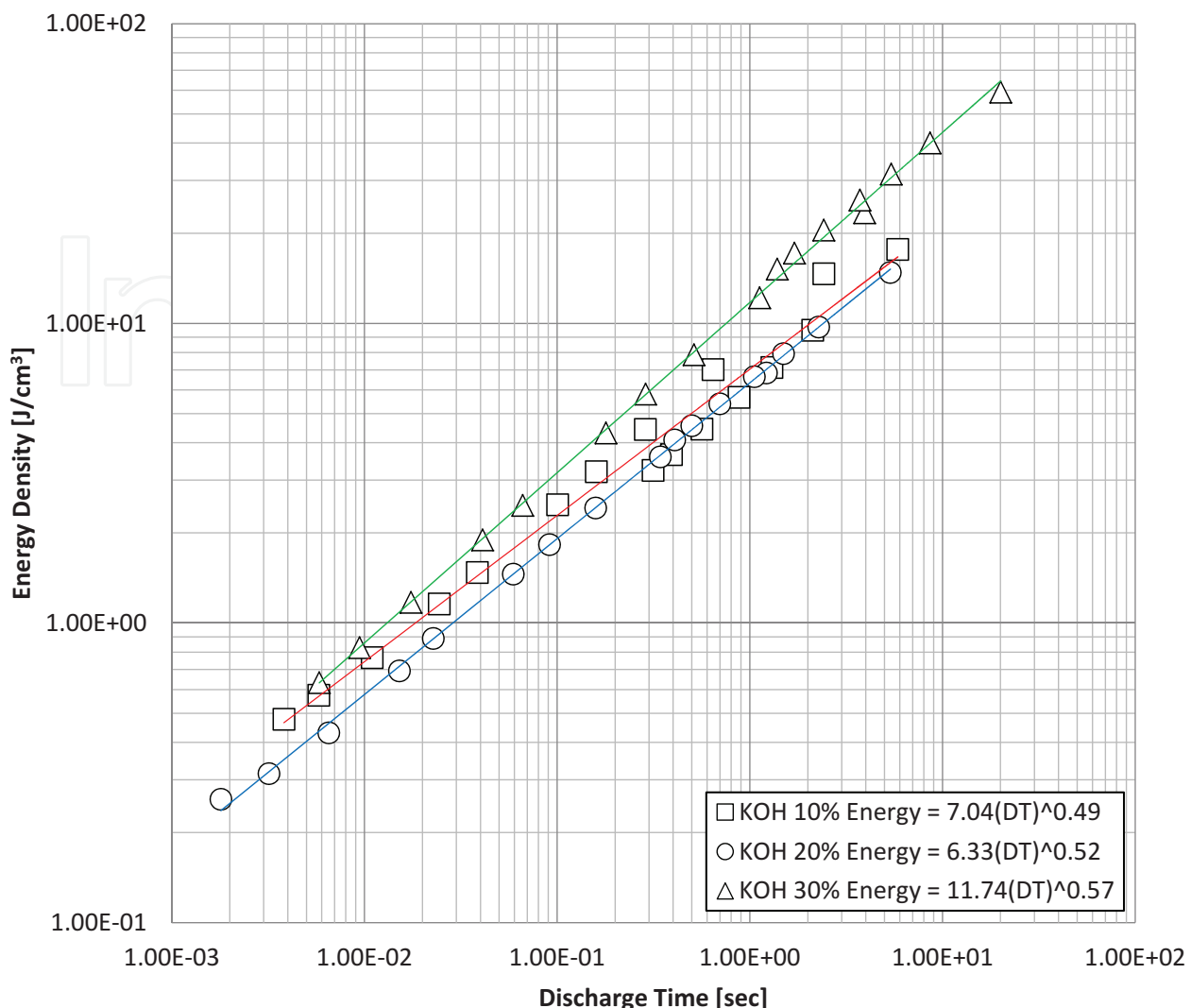


**Figure 2.** Energy density vs. discharge time for KOH-based capacitors. At all three KOH concentrations, the energy density ‘rolls off’ as a very specific function of discharge time. This allows determination of energy density with high precision over a broad discharge time range. Note the curve slope increases, and the energy density at all concentrations increases with increasing solute concentration. Employing the linear fitting equations with DT, in seconds, yields energy in J/cm<sup>3</sup>.

for many pulsed power applications. The data for NaNO<sub>3</sub> and NH<sub>4</sub>Cl are only shown in a figure representing a summary of all nine capacitors. Greater detail is available elsewhere [24].

Capacitance as a function of discharge time for all three KOH-based systems is shown in **Figure 4**. These values were computed directly from the slope of the curves below ~0.8 V (**Figure 1**) and hence are only valid below this value. Despite this limitation, the data are of interest as it shows remarkably high values for very small volume systems.

It is notable that none of the parameters, including capacitance, show a clear pattern with salt concentration. The fact that key parameters do not track with salt concentration has been noted with all other SDM-based capacitors [9–13].

The final parameter of interest is the dielectric constant, generally an excellent engineering value as it permits the selection of capacitors, based on this single number, with a high degree

Solute (wt%)	Dielectric constant<0.8V		Energy density (J/cm <sup>3</sup> )		Power density (Watt/cm <sup>3</sup> )	
	10 s	1000 s	10 s	1000 s	0.01 s	
KOH (10)	1.1 E+8	7.3 E+8	22	208	74	
KOH (20)	1.2 E+8	1.0 E+9	21	230	58	
KOH (30)	2.1 E+8	1.8 E+9	44	602	85	
NH <sub>4</sub> Cl (10)	2.7 E+8	4.1 E+9	35	556	56	
NH <sub>4</sub> Cl (20)	2.2 E+8	2.9 E+9	30	356	72	
NH <sub>4</sub> Cl (30)	2.1 E+8	1.9 E+9	34	363	98	
NaNO <sub>3</sub> (10)	1.3 E+7	9.8 E+7	4	23	26	
NaNO <sub>3</sub> (20)	3.1 E+7	3.0 E+8	12	125	37	
NaNO <sub>3</sub> (30)	3.0 E+7	2.8 E+8	12	142	36	

The values at 10 s (discharge time) are in the measured range. The values at 1000 s are extrapolated values based on using the power law fits.

**Table 1.** Select parameters.

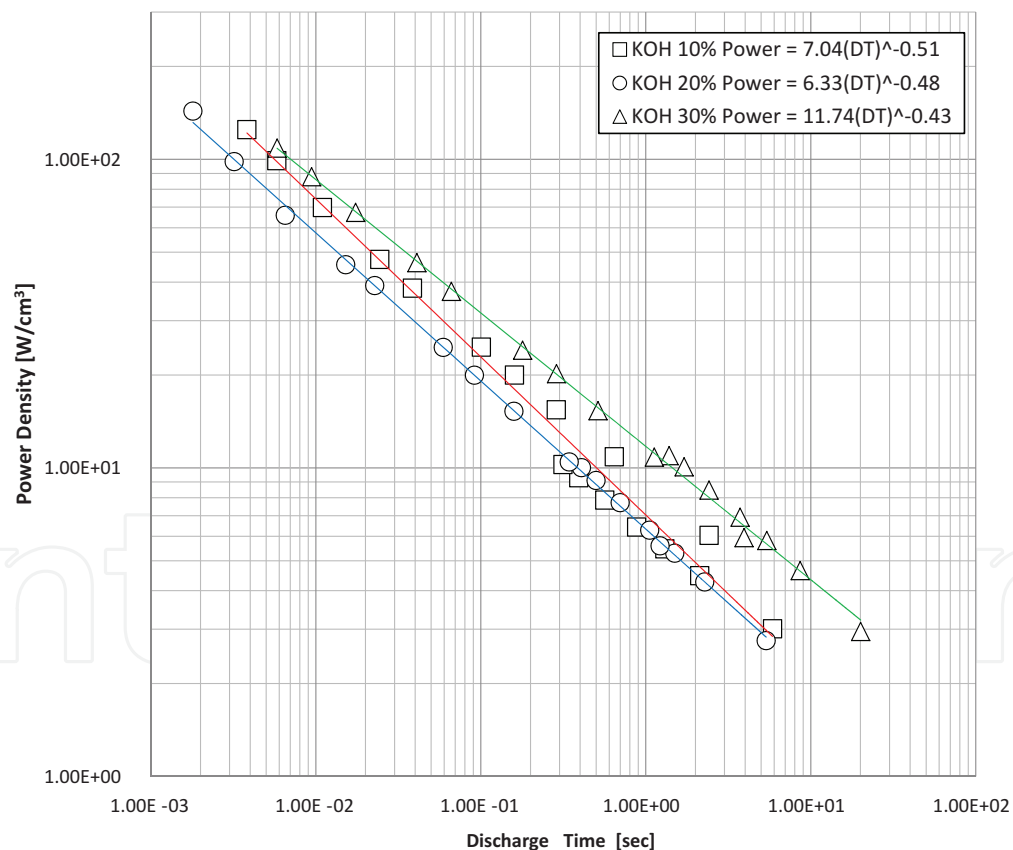


**Figure 3.** Power density vs. discharge time for KOH-based capacitors. At all three KOH concentrations, the power density increases with decreasing discharge time. The data clearly follow a simple power law in all cases, permitting determination of power density with high precision over a broad discharge time range. Employing the linear fitting equations, with DT, in s, yields power in W/cm<sup>3</sup>.

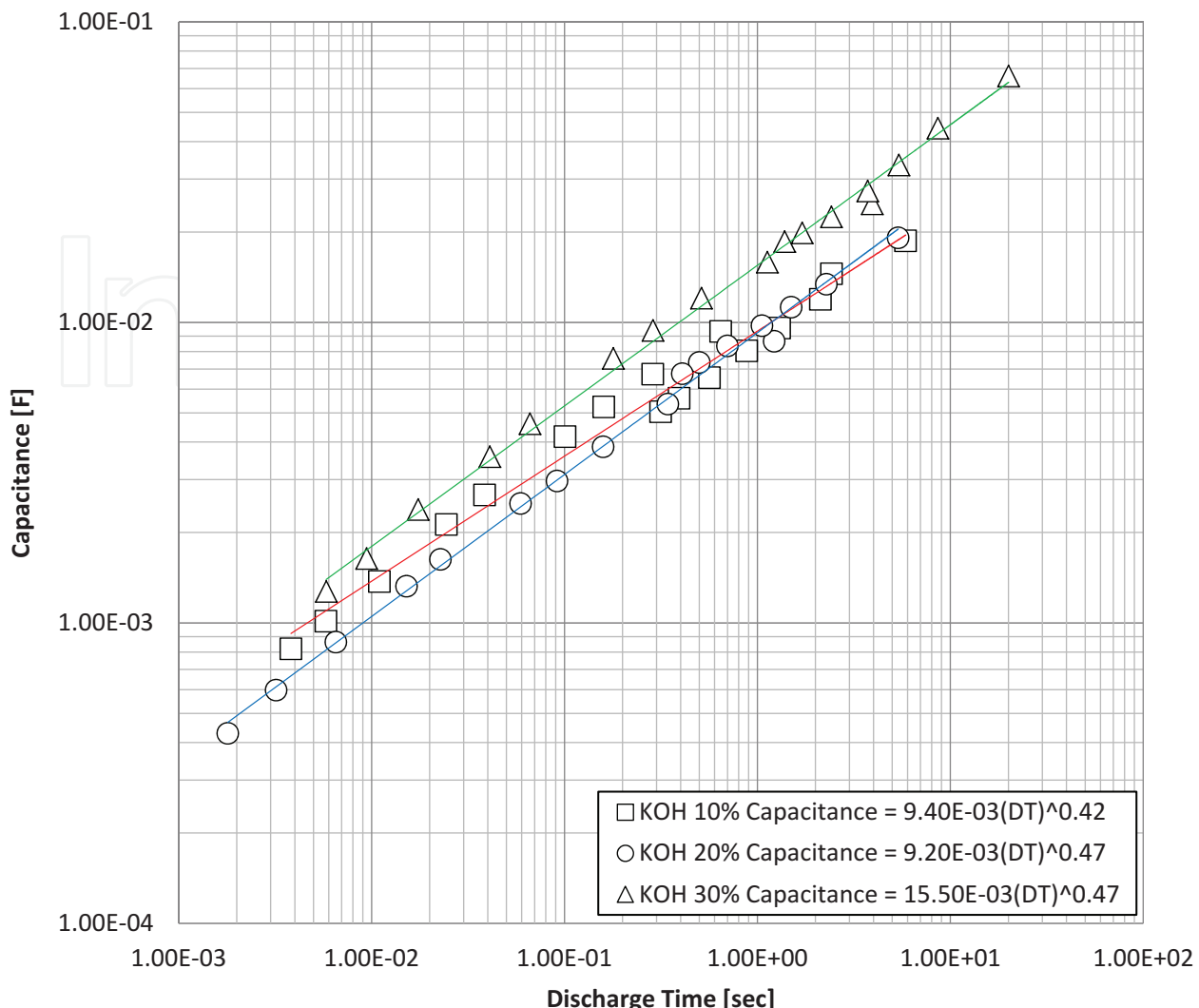


**Figure 4.** Capacitance vs. discharge time for KOH-based capacitors. At all three KOH concentrations, the capacitance clearly follows a simple power law in all cases, permitting determination of its value with high precision over a broad discharge time range.

of certainty they will perform as anticipated. However, for SDM-based capacitors employed for energy storage, for which dielectric constant is not a constant of voltage or frequency, it is not a quantitative predictor of performance. Notably, the dielectric constant also does not serve any role in rating EDLC for which dielectric constants in the traditional sense cannot really be measured. In fact, for EDLC a dielectric constant with units,  $\text{F}/\text{cm}^2$  is the only 'dielectric' value cited [31–34]. Still, there are two good reasons for measuring and reporting this value. First, it provides a qualitative predictor of energy and power density. Second, the values (**Figure 5**) permit a quantitative comparison with the historic database of dielectric materials, including other super dielectric materials. For example, the far greater values of dielectric constants for SDM below ~1 V, generally more than  $10^5$  greater than any solid dielectric, show them to be a distinct class of materials.

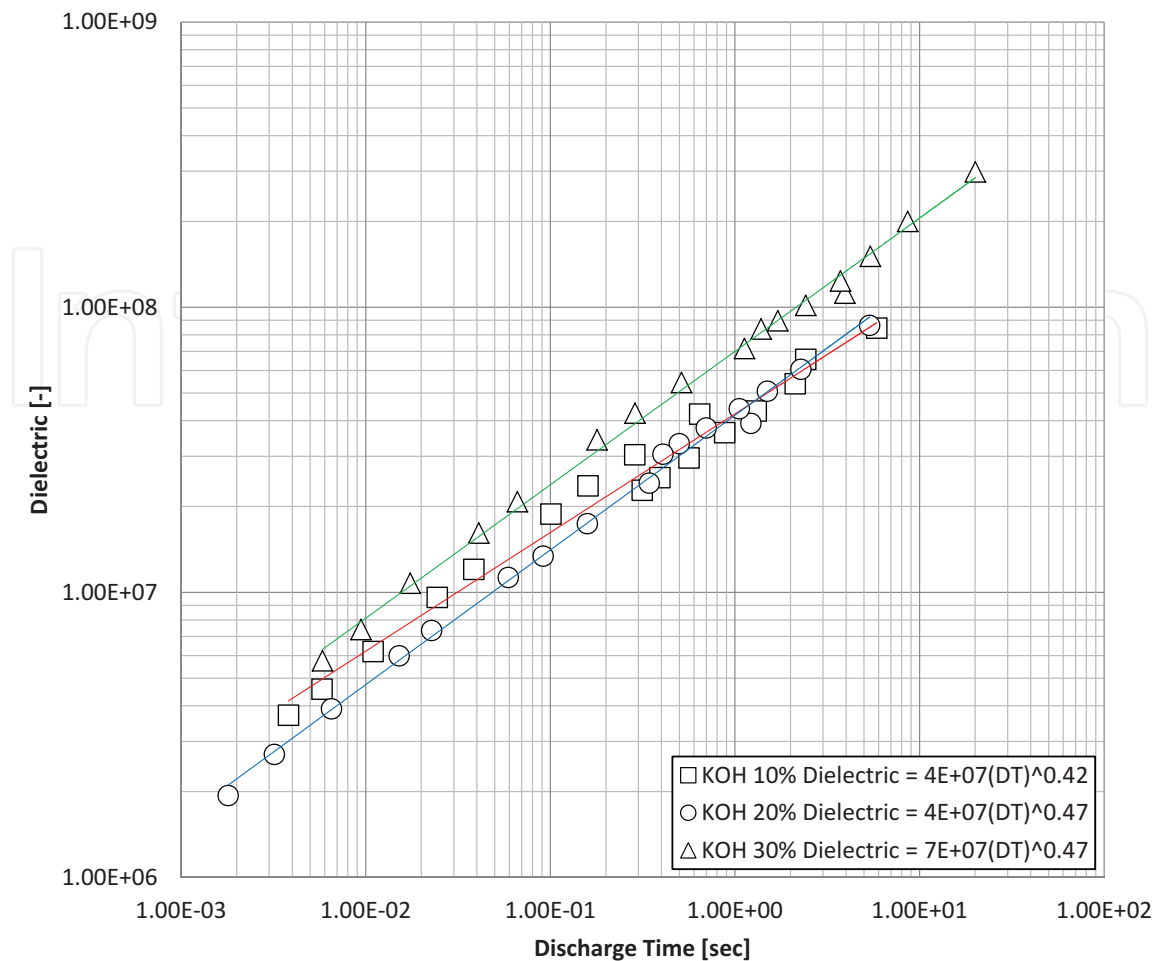


**Figure 5.** Dielectric constant vs. discharge time for KOH-based capacitors. At all three KOH concentrations, the dielectric constant follows, below ~0.8 V, a simple power law, permitting determination of its value with high precision over a broad discharge time range. The absolute values of the dielectric constant are greater than  $10^6$  even at a discharge time of order  $10^{-3}$  s, indicating these materials were super dielectric materials over the full range tested.

### 3.3. $\text{NH}_4\text{Cl}$

The only complete data set shown for the aqueous  $\text{NH}_4\text{Cl}$ -based dielectric is the dielectric constant as a function of discharge time (**Figure 6**). The values of this parameter are similar to those of the aqueous KOH-based dielectrics and the other values are as well. Only dielectric constant is displayed as this parameter is most easily compared to the historic data set of dielectric materials. It is also notable that the data derived from aqueous  $\text{NH}_4\text{Cl}$  solutions show greater variability than data from capacitors made with either of the other solutions.

### 3.4. $\text{NaNO}_3$

For the aqueous  $\text{NaNO}_3$ -based dielectric, the only complete data set provided is the dielectric constant as a function of discharge time (**Figure 7**). The values of this parameter are distinctly less, on the order of a factor of five at any given discharge time, than those

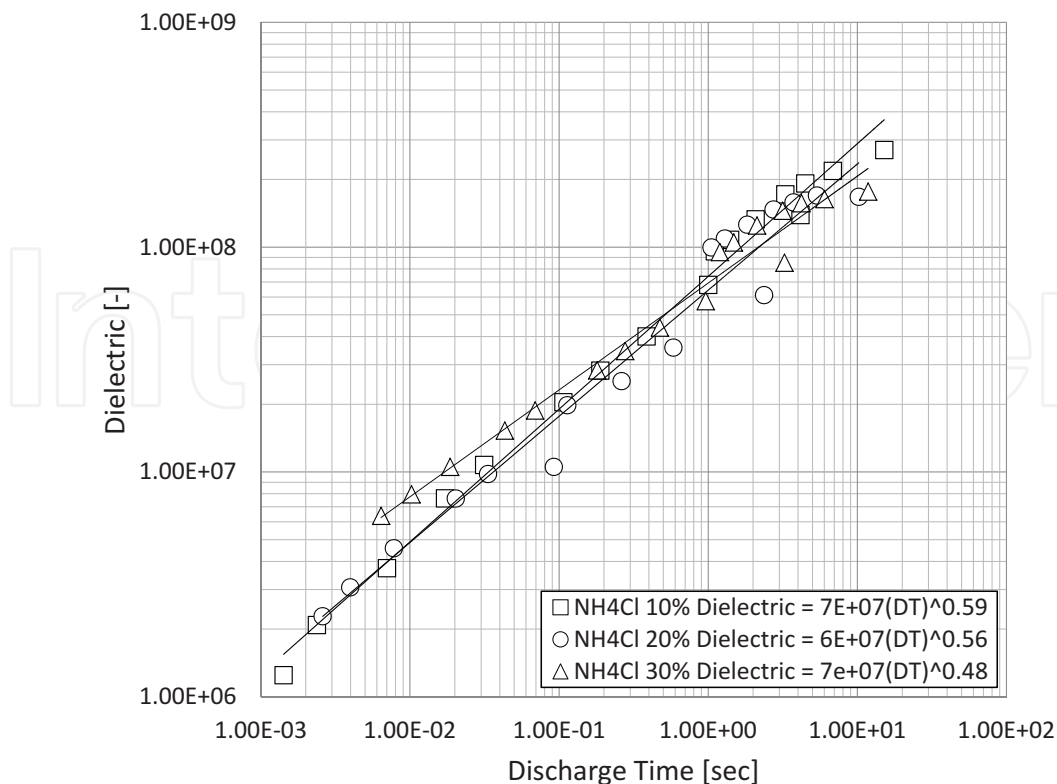


**Figure 6.** Dielectric constant vs. discharge time for NH<sub>4</sub>Cl-based capacitors. At all three NH<sub>4</sub>Cl concentrations, the dielectric constant follows, below ~0.8 V, a simple power law. The absolute values of the dielectric constant are similar to those of KOH at all discharge times, and greater than 10<sup>6</sup> even at a discharge time of order 10<sup>-3</sup> s, indicating these materials were super dielectrics over the full range tested.

observed for both the aqueous KOH- and NH<sub>4</sub>Cl-based dielectrics. This is a qualitative indicator that the energy and power density of capacitors built T-SDM employing this solution will not perform as well for storing energy and providing power. This is shown to be true in the next section.

### 3.5. Energy and power

The energy density for all three aqueous salt solutions with 30 wt% concentration is shown in **Figure 8**. The energy density for two of these solutions, KOH and NH<sub>4</sub>Cl, are very similar across the entire range of discharge times collected. This is consistent with the observations that they have very similar dielectric values over the same tested time range. The energy density of the capacitors employing NaNO<sub>3</sub> is less than a third the value of capacitors built using either of the other two solutions at any given frequency and also qualitatively consistent with the relatively low dielectric value of this solution. Also notable is the clear indication that the method does not provide reliable data for discharge times less than approximately 0.001 s. At this high rate of discharge, the method does not capture a sufficient number of data points to provide a reliable integrated energy density.

A comparison of the power density for the three capacitors built with 30 wt% salt solutions is shown in **Figure 9**. Once again, the KOH and NH<sub>4</sub>Cl behavior is very similar, as anticipated

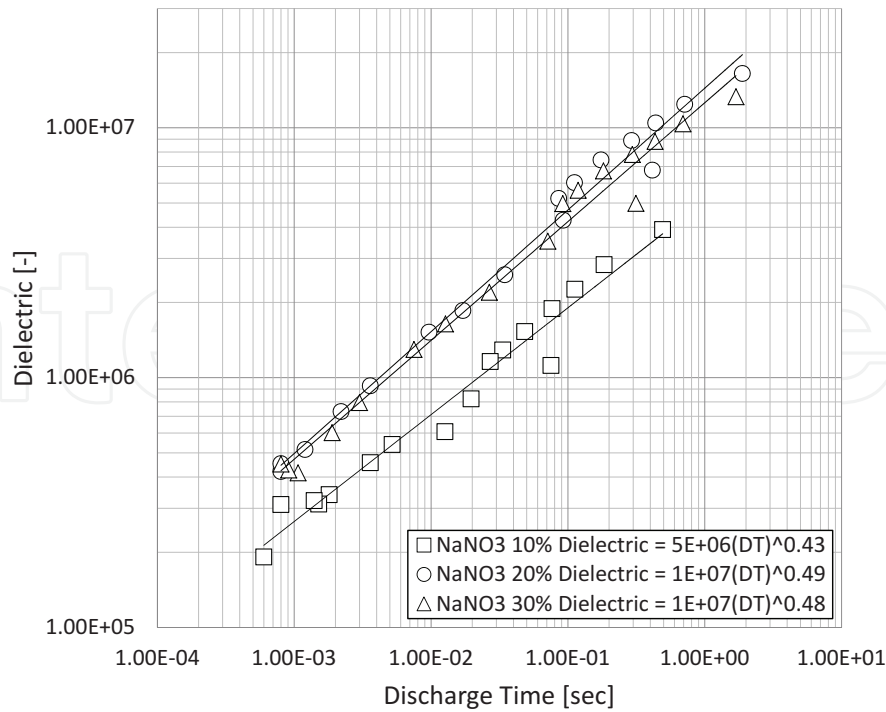


**Figure 7.** Dielectric constant vs. discharge time for NaNO<sub>3</sub>-based capacitors. At all three concentrations, the dielectric constant follows, below ~0.8 V, a simple power law. The absolute values of the dielectric constant are about an order of magnitude less than the KOH and NH<sub>4</sub>Cl-based capacitors at any given discharge time. Still, at all discharge times tested the dielectric constant was greater than 10<sup>5</sup>, indicating these materials were super dielectrics over the full range tested.

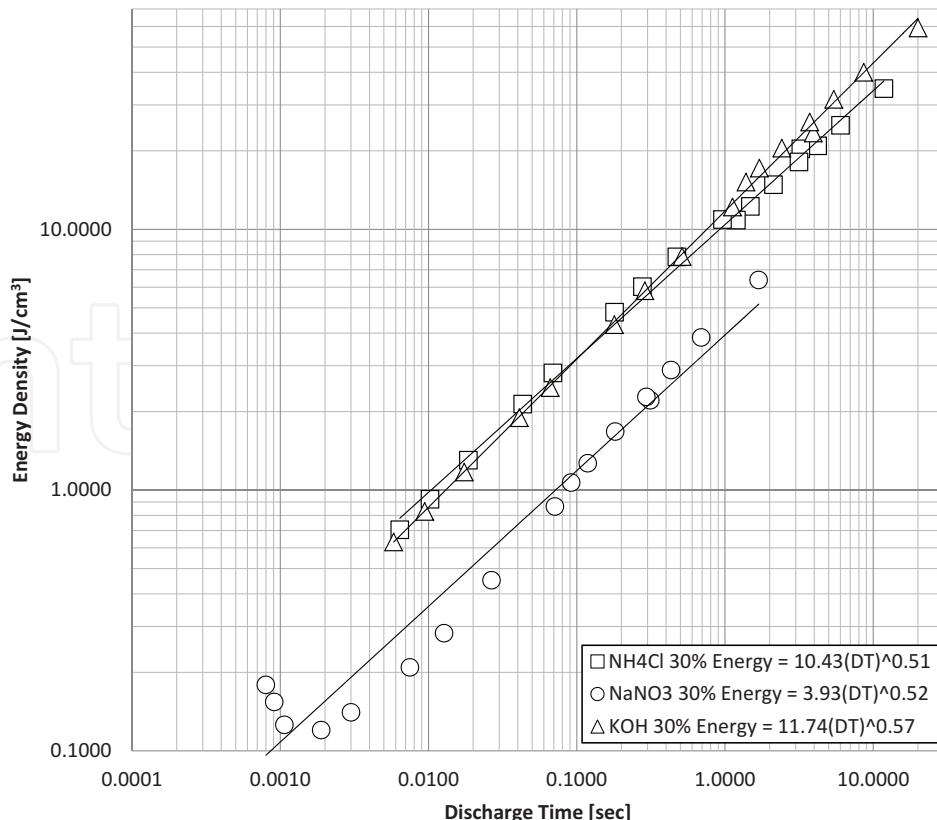


**Figure 8.** Energy density comparisons. The energy density for capacitors built with three different 30 wt% salt solutions is shown over more than three orders of magnitude of discharge time. The data below 0.001 s discharge time are considered inaccurate due to insufficient data collection times.

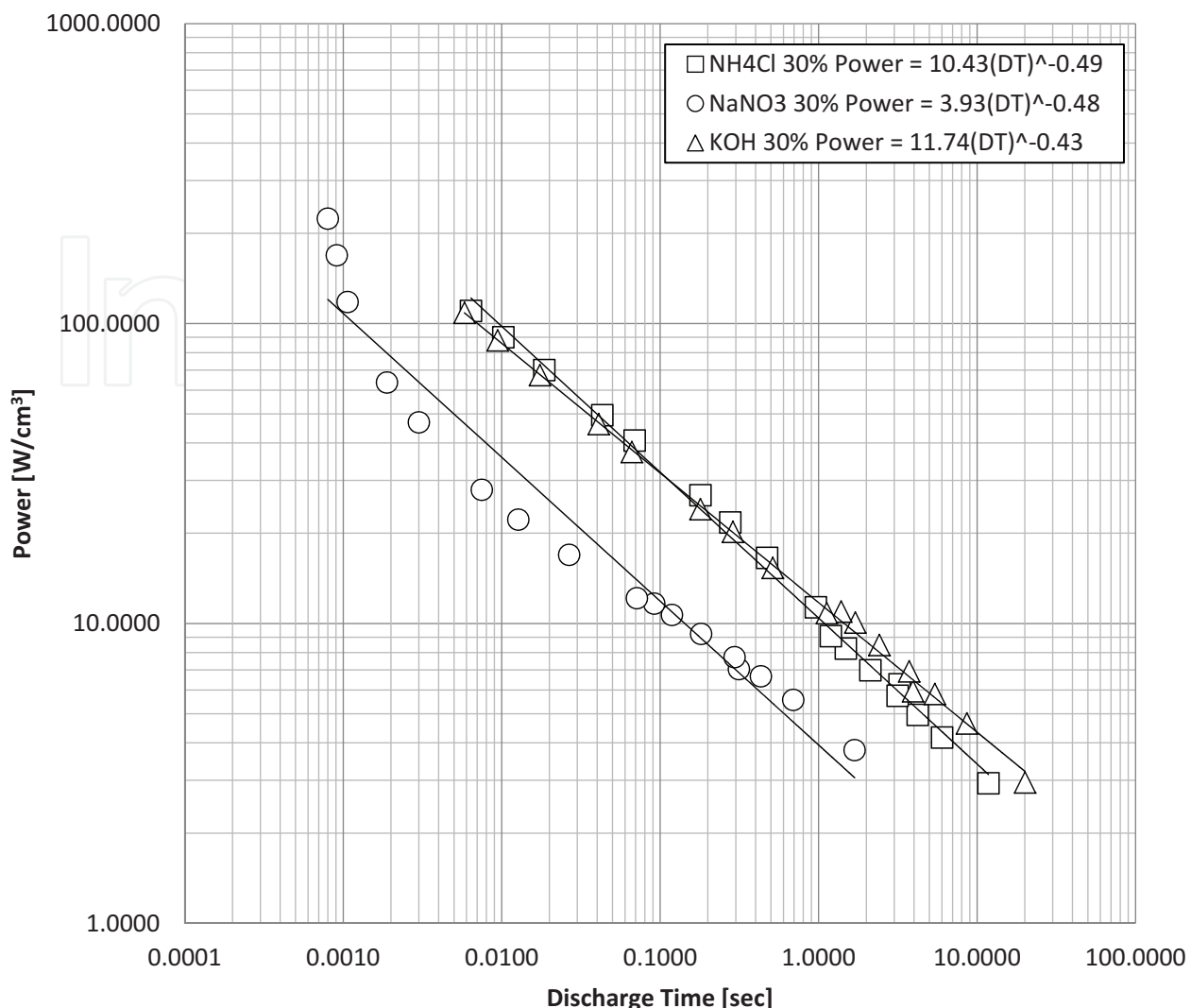


**Figure 9.** Power density comparisons. The power density for capacitors built with three different 30 wt% salt solutions is shown over more than three orders of magnitude of discharge time.

based on the similarity in the reported dielectric values over the full range of discharge times studied. It is also clear that the aqueous  $\text{NaNO}_3$  capacitor yields the lowest power densities, by a factor of approximately three at all discharge times, as expected given the lower dielectric values reported. Although not shown here, the relative energy and power densities observed for the 30% solutions are exemplary of the relative values of these parameters at all concentrations.

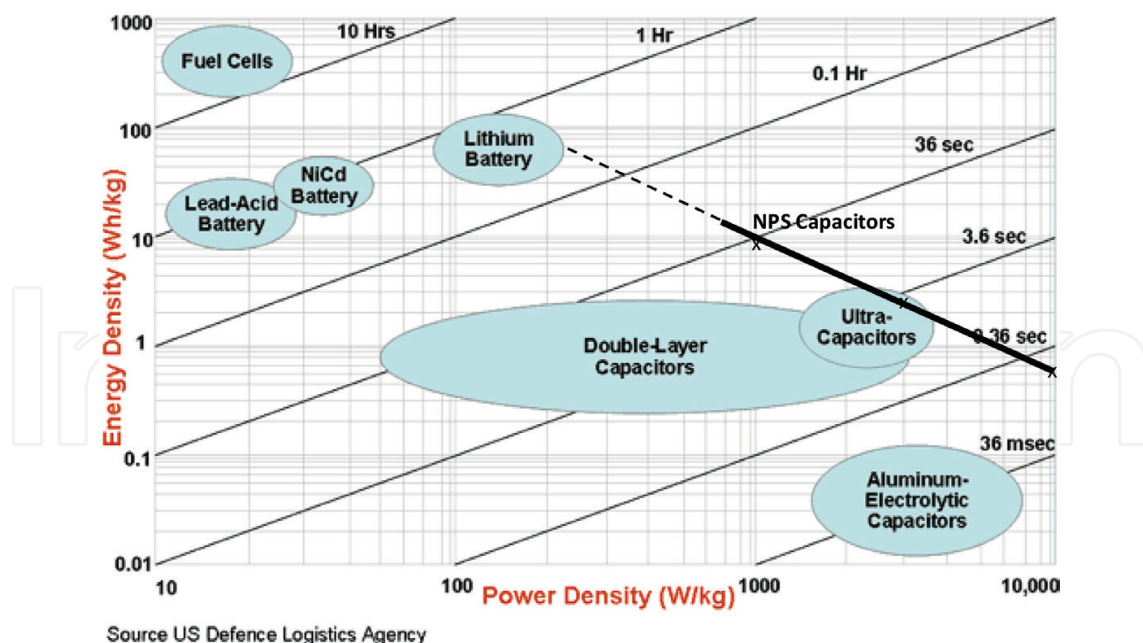
#### 4. Discussion

The following were observed for all nine ion capacitors containing dissolved ions: (i) All the capacitors displayed 'roll-off' of capacitance (<0.8 V), dielectric constant (<0.8 V), and energy density (0.1–2.3 V) as discharge time decreased. (ii) The roll-off, of all these parameters, is well described by simple power law expressions derived from data covering more than three orders of magnitude of discharge times. (iii) Power density is also well described by a simple power law, but in contrast to all other parameters of interest, increased in all

cases as the discharge time was reduced. (iv) The identity and concentrations of the solutes had a strong impact on the value of all capacitor performance parameters. (v) The value of all parameters was not a clear function of solute concentration, although the highest weight concentration, 30%, performed the best. (vi) In general, capacitors based on KOH and NH<sub>4</sub>Cl were similar in behavior, but the NaNO<sub>3</sub>-based capacitors consistently showed the lowest values.

The data presented herein provide the first report on the behavior of T-SDM as a function of discharge time. This information is critical for assessing the value of any type of capacitor for application to 'pulsed power'. Indeed, the measured power densities, just greater than 100 W/cm<sup>3</sup> for both the aqueous KOH- and NH<sub>4</sub>Cl-based capacitors, for discharges of 0.01 s, are exceptional. As shown in **Figure 10**, the KOH-based capacitor parameters fall above the 'range' of operation anticipated for EDLC-based supercapacitors and are far better than the performance determined using the identical methodology employed in this work to assess real commercial 'supercapacitors' [24] in our laboratory. Three supercapacitors were tested and the best passed through the bottom range of values anticipated by the plot shown (**Figure 10**), and the other two were completely below the 'bubble' of performance anticipated for 'double layer capacitors'.

It is also important to compare the data obtained in this study with earlier work on T-SDM. That earlier work was undertaken with a different objective: Study very slow discharges (>1000 s) appropriate for determining their potential use of T-SDM as energy storage devices. The



Source US Defence Logistics Agency

**Figure 10.** KOH 30 wt% NPS energy/power performance. On a modified US Defense Logistics Agency Ragone chart, it is clear that the 30 wt% KOH-based capacitor (solid line) is superior to that anticipated for EDLC or double layer capacitors. Also, the data fall on a line, which can reasonably be extrapolated using the power law fits (dashed curve). It was assumed that the dielectric is half salt water and half titania with density 2.6 g/cm<sup>3</sup>.

measured energy densities reported herein, for both KOH- and NH<sub>4</sub>Cl-based capacitors, are comparable to the values obtained in prior studies. Those were obtained using a different solution, 30% NaCl, and a different measurement method, the traditional RC time constant method. In fact, using the simple power law dependencies obtained here and extrapolating to 1000 s, the energy density is a remarkable ~600 J/cm<sup>3</sup>. In the earlier RC time constant work a nearly identical titania matrix containing 30 wt% NaCl aqueous solution yielded nearly 400 J/cm<sup>3</sup> for similar discharge times. Given the different ionic solutions, the different measurement protocols and other minor differences, there is an excellent agreement between the two studies.

The basic model of T-SDM presented elsewhere [7, 8, 10] predicts high capacitance that decrease as the discharge time decreases. To understand both, a brief review of the static model of SDM and a qualitative review of the dynamics of SDM is required. Regarding the former: As illustrated by the cross-section model of an anodized titania filled with aqueous solution, **Figure 11**, dipoles created by the movement of ions in solution toward oppositely polarized electrodes create ‘giant dipoles’. These dipoles, opposite in polarization to the electrodes, reduce the field, everywhere, created by charges on the electrodes. As voltage is the line integral of field from ground to electrode, the lowering of field everywhere reduces the voltage. Thus, it takes more charge on the electrodes to reach the same voltage when these giant dipoles are fully (static conditions) aligned. More charge, at the same voltage, means a higher capacitance, by definition. In essence, dipole formation is the basis for capacitance enhancement for all types of dielectrics; however, for SDM the dipoles are orders of magnitude longer than in any solid so the field reduction, and consequently the increase in capacitance, is more dramatic. Next, it is necessary to reflect on the dynamics of dipole formation, that is the impact of frequency, or period, on dipole strength. Specifically, if the electrode polarization is switched too quickly for the ions in solution to ‘swim’ to the maximal (static) dipole positions, the net or effective, dipole length, and concomitantly the dielectric and capacitance values, are reduced. The

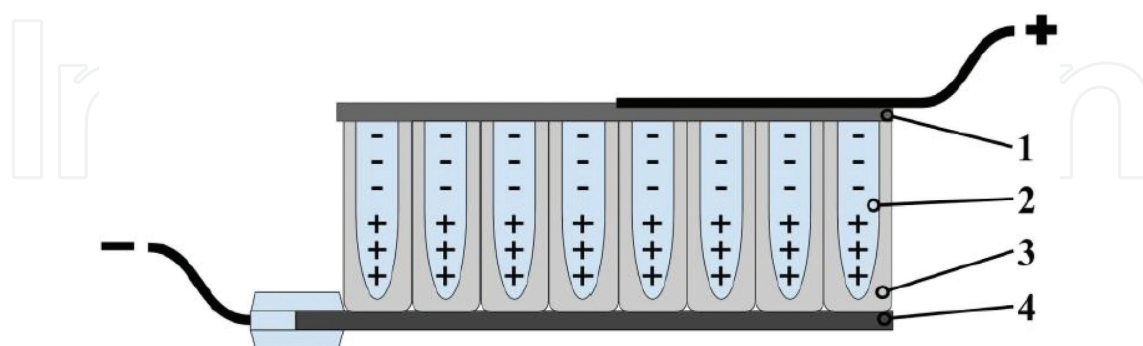


**Figure 11.** X-Section model of dipole formation in SDM. 1. Top electrode, Grafoil. 2. Tube filled with aqueous ion solution. 3. 90 nm × 8 μm titania tubes formed by anodization. 4. Titanium metal electrode. Upon the application of a field, the ions in solution migrate to form dipoles oppositely polarized to the electrodes. The effective dipole strength in the dielectric is a function of time. Given sufficient time (static) dipoles of maximum length and charge separation form. The effective dipole length/strength is a function of net length and thus is discharge time/frequency dependent.

data suggest that effective dipole length follows a very simple pattern as a function of discharge time.

It is notable that this is only the second time [13] the constant current charge/discharge method has been employed to determine the power law relationship for 'supercapacitor' parameters, specifically capacitance, dielectric constant, and energy and power density, over orders of magnitude of discharge times. This method arguably provides higher fidelity, more reliable, insight into 'frequency' dependence of this type of capacitor than other measurement protocols.

## 5. Conclusions

This study establishes, empirically, that T-SDM capacitors, based on dielectrics created by filling micron scale titania tubes that form during titanium ionization with aqueous salt solutions, are superior to all other energy storage capacitors, relative to standard metrics. Using a recently developed constant current protocol, it was demonstrated that the capacitance, dielectric constant, and energy and power density as a function of discharge time follow power law relationships. Plotted on a Ragone chart, the power vs. energy density data is linear. All data lie above the values recorded for supercapacitors, ultra capacitors, and electrolytic capacitors on standard Ragone charts. Furthermore, the consistency of the data, that it resulted in power law relationships for capacitors derived from nine different salt solutions, indicates that the data and the fitted power laws are precise and are probably accurate. Notably, dielectric constants of more than  $10^8$  were recorded, and even for very short discharges for all capacitors, the dielectric constant was  $>10^5$ , establishing that the dielectrics are SDM over a broad range of discharge times (ca.  $10^{-3}$ – $>10$  s). Finally, it should be noted that the measured power delivery increases as the discharge time decreases. For three of the capacitors, the measured power delivery was greater than  $70\text{ W/cm}^3$  for a 10 ms discharge, a time frame and a power delivery value consistent with the needs of pulsed power systems.

## Author details

Steven M. Lombardo and Jonathan Phillips\*

\*Address all correspondence to: jphillip@nps.edu

Naval Postgraduate School, Monterey, CA, USA

## References

- [1] Christen T, Carlen W. Theory of Ragone plots. Journal of Power Sources. 2000;91:210

- [2] Ragone D. Review of battery systems for electrically powered vehicles. SAE Technical Paper 680453. 1968. DOI: 10.4271/680453
- [3] Simon P, Gogotsi Y. Materials for electrochemical capacitors. *Nature Materials*. 2008;7:845
- [4] Dato A, Radmilovic V, Lee Z, Phillips J, Frenklach M. Substrate-free gas-phase synthesis of graphene sheets. *Nano Letters*. 2008;8:2012-2016
- [5] El-Kady MF, Strong V, Dubin S, Kaner RB. Laser scribing of high-performance and flexible graphene-based electrochemical capacitors. *Science*. 2012;335:1326
- [6] Shao Y, El-Kady MF, Wang LJ, Zhang Q, Li Y, Wang H, Mousavi MF, Kaner RB. Graphene-based materials for flexible supercapacitors. *Chemical Society Reviews*. 2015;44:3639
- [7] Yang X, Zhuang X, Huang Y, Jiang J, Tian H, Wu D, Zhang F, Mai Y, Feng X. Nitrogen-enriched hierarchically porous carbon materials fabricated by graphene aerogel templated Schiff-base chemistry for high performance electrochemical capacitors. *Polymer Chemistry*. 2015;6:1088-1095
- [8] Gandy J, Quintero F, Phillips J'. Testing the tube super dielectric material hypothesis: Increased energy density using NaCl. *Journal of Electronic Materials*. 2016;45:5499
- [9] Quintero F, Phillips J. Tube-super dielectric materials: Electrostatic capacitors with energy density greater than  $200 \text{ J}\cdot\text{cm}^{-3}$ . *Materials*. 2015;8:6208-6227
- [10] Fromille S, Phillips J. Super dielectric materials. *Materials*. 2014;7:8197-8212
- [11] Quintero F, Phillips J. Super dielectrics composed of NaCl and  $\text{H}_2\text{O}$  and porous alumina. *Journal of Electronic Materials*. 2015;44:1367
- [12] Jenkins N, Petty C, Phillips J. Investigation of fumed aqueous NaCl superdielectric material. *Materials*. 2016;9:118
- [13] Phillips J. Novel superdielectric materials: Aqueous salt solution saturated fabric. *Materials*. 2016;9:918
- [14] J Phillips, SS Fromille. Superdielectric materials US Patent 9,530,574 (2016)
- [15] Kao KC. *Dielectric Phenomena in Solids: With Emphasis on Physical Concepts of Electronic Processes*. Academic Press; New York, NY USA. 2004
- [16] Debye PJW. *Polar Molecules*. Chemical Catalog Company, Incorporated; New York, NY USA. 1929
- [17] Onsager L. Electric moments of molecules in liquids. *Journal of the American Chemical Society*. 1936;58:1486
- [18] Kim CH et al. Tailoring the pore structure of carbon nanofibers for achieving ultrahigh-energy-density supercapacitors using ionic liquids as electrolytes. *Journal of Materials Chemistry A*. 2016;4:4763

- [19] Xu Y, Lin Z, Zhong X, Huang X, Weiss NO, Huang Y, Duan X. Holey graphene frameworks for highly efficient capacitive energy storage. *Nature Communications*. 2014;**5**:4554. DOI: 10.1038/ncomms5554
- [20] Sahu V et al. Ultrahigh performance supercapacitor from lacey reduced graphene oxide nanoribbons. *ACS Applied Materials and Interfaces*. 2015;**3110**(2015):7
- [21] Zwilling V, Darque-Ceretti E, Boutry-Forveille A, David D, Perrin MY, Aucouturier M'. Structure and physicochemistry of anodic oxide films on titanium and TA6V alloy. *Surface and Interface Analysis*. 1999;**27**:629
- [22] Roy P, Berger S, Schmuki P'. TiO<sub>2</sub> nanotubes: Synthesis and applications. *Angewandte Chemie, International Edition*. 2011;**50**:2904
- [23] Cortes FJQ, Arias-Monje PJ, Phillips J, Zea H. Empirical kinetics for the growth of titania nanotube arrays by potentiostatic anodization in ethylene glycol. *Materials & Design*. 2016;**96**:80-89
- [24] Lombardo SM. Characterization of Anodized Titanium-Based Novel Paradigm Supercapacitors: Impact of Salt Identity and Frequency on Dielectric Values, Power and Energy Densities. M.S. Thesis, Naval Postgraduate School; 2016
- [25] Phillips J, Clausen B, Dumesic JA. Iron pentacarbonyl decomposition over grafoil. Production of small metallic iron particles. *The Journal of Physical Chemistry*. 1980;**84**:1814
- [26] Phillips J, Dumesic JA. Iron pentacarbonyl decomposition over grafoil: II. Effect of sample outgassing on decomposition kinetics. *Applied Surface Science*. 1981;**7**:215-230
- [27] Barsoukov E, MacDonald JR. Impedance Spectroscopy: Theory, Experimental and Applications. 2nd ed. New York, NY, USA: John Wiley & Sons; 2005
- [28] MacDonald JR, Kenan WR. Impedance Spectroscopy. Emphasizing Solid Materials and Systems. New York, NY, USA: John Wiley & Sons; 1987
- [29] Kim Y, Kathaperumal M, Chen VW, Park Y, Fuentes-Hernandez C, Pan MJ, Kippelen B, Perry JW. Bilayer structure with ultrahigh energy/power density using hybrid sol-gel dielectric and charge-blocking monolayer. *Advanced Energy Materials*. 2015;**5**:1500767. DOI: 10.1002/aenm.201500767
- [30] Gogotski Y, Simon P. True performance metrics in electrochemical energy storage. *Science*. 2011;**334**:917
- [31] Conway BE. Electrochemical Supercapacitors: Scientific Fundamentals and Technological Applications. Springer Science and Business Media; New York, NY USA. 1999
- [32] Simon P, Burke AF. Nanostructured carbons: Double-layer capacitance and more. *Electrochemical Society Interface*. 2008:38-43
- [33] Ji H et al. Capacitance of carbon-based electrical double-layer capacitors. *Nature Communications*. 2014;**5**:3317
- [34] Reynolds GJ, Krutzer M, Dubs M, Felzer H, Mamazza R'. Electrical properties of thin-film capacitors fabricated using high temperature sputtered modified barium titanate. *Materials*. 2012;**5**:644